Received: 4 August 2019
DOI: 10.1002/mma.7056

SPECIAL ISSUE PAPER

WILEY

Application of surface growth model for a pathological process in a blood vessel's wall

Evgenii V. Murashkin[1] | **Evgeniy P. Dats**[2,3] | **Nikita E. Stadnik**[1,4]

[1]Laboratory of Modelling in Solid Mechanics, Ishlinsky Institute for Problems in Mechanics of the Russian Academy of Sciences, Moscow, Russia

[2]Department of Computational Informatics, Institute of Applied Mathematics of the Far Eastern Branch of the Russian Academy of Sciences, Vladivostok, Russia

[3]Department of Mathematics and Modelling, Vladivostok State University of Economics and Service, Vladivostok, Russia

[4]Faculty of Paediatrics, Federal State Autonomous Educational Institution of Higher Education I.M. Sechenov First Moscow State Medical University of the Ministry of Health of the Russian Federation (Sechenov University), Moscow, Russia

Correspondence
Evgenii V. Murashkin, Ishlinsky Institute for Problems in Mechanics of the Russian Academy of Sciences, Moscow, Russia.
Email: evmurashkin@gmail.com

Communicated by: T. E. Simos

Funding information
Russian Foundation for Basic Research, Grant/Award Number: 19-51-60001 and 20-01-00666

The present study deals with a problem of modeling a surface growth process. Governing principles for mechanics of growing solids have been formulated. Within the framework of the surface growth theory, different variants of boundary value problems are discussed. A human blood vessel under pathological growth processes has been considered as an example of a surface growth process. Vessels are simulated by a long thick-walled circular cylinder. The boundary value problem of a surface growth for elastic thick-walled vessels is solved. The analytical solution in terms of velocities for parameters of stress-strain state has been obtained. Condition of thickness has allowed us to study strain-stress state of cylinder surfaces using approximation of infinitesimal deformations. The stress-strain state characteristics are numerically computed and graphically analyzed using various mechanical parameters of the surface growth processes. Two cases of boundary value problems, namely, deformation of two- and multilayer cylinder have been considered. General analytical solution for thick multilayer cylinder deformation has been obtained. Analytical solution is based on the Lamé problem for elastic material. Comparison of multilayer and single-layer solutions is performed.

KEYWORDS
blood vessel wall, composite cylinders, elastic deformation, growing solids, residual stress, surface growth

MSC CLASSIFICATION
74B10; 74M15; 74L15; 92C10; 35Q74

1 | INTRODUCTION

1.1 | Medicine problems coupled with growth processes

Human and animal organs can be morphologically divided into two types. The first type consisting of parenchyma and stroma is called parenchymal organs. These include, for example, liver, brain and spinal cord, and pancreas. The second

Nomenclature: α_i, ratio of Young's moduli; ∇, nabla operator; $\boldsymbol{\sigma}, \sigma_{ij}$, stress tensor; γ_i, sum of Lamé parameters; λ_i, μ_i, Lamé parameters; ν_i, Poison's ratio; $\overset{*}{\Sigma}(t)$: $t = \overset{*}{\tau}(\mathbf{x})$, propagating growing surface; ∂_t, time derivative; A_i, B_i, X_i, Y_i, unknown integrating constants; E_i, Young's modulus; R_i, radii of a cylinder; s_n, normal velocity of the growing surface Σ; $\mathbf{D}, D_{ij}$, strain rate tensor; $\mathbf{e}, e_i$, strain tensor; $\mathbf{L}$, 2D curvature tensor on the surface Σ; $\mathbf{n}$, unit normal vector on the surface Σ; $\mathbf{u}, u_k$, displacement vector; $\mathbf{v}, v_k$, velocity vector; $\mathcal{T}_s$, 2D tensor of the given elastic growing surface tension.

type is tubular (layered) organs. They are a cavity with walls, for example, blood vessels, bronchial tubes, bile ducts, and gastrointestinal tract. Cells in such organs are arranged in layers and, as a rule, form three shells: tunica intima, tunica media and tunica adventitia. As a typical tubular organ, wall of a large blood vessel (like arteries or veins) structurally consists of these three shells. The outer shell (tunica adventitia) is the thickest layer in veins, which is entirely made of connective tissues. The middle shell (tunica media) is the thickest layer in arteries. It is presented by smooth muscle cells. The inner membrane is the thinnest layer presented by a flat single-layer epithelium lying on the basal membrane.[1-5] There are many pathological processes leading to obturation of a lumen of a tubular organ due to the deposition of particles on a surface or proliferation.[6]

The remodeling of the vessel's wall by virtue of a volumetric wall thickening is an example of pathological volumetric growth, which can be mathematically simulated by the volumetric growth models. Elastosis and elastofibrosis are revealed in the arteries of large and medium diameter under high blood pressure (hypertension). These processes are sequential stages of a pathological process, and both are hyperplasia and cleavage of the internal elastic membrane. They progress as a compensatory response to a persistent increase of blood pressure. Further, the destruction of elastic fibers occurs, and they are replaced by collagen fibers, i.e., sclerosis. Thus, the walls of vessels are thickened, and the lumen is narrowed.[7,8]

The present study deals with two pathological processes of atherosclerotic lesions of arteries and thrombosis of veins.[9,10] These processes can be mathematically simulated by the volumetric growth models.

Every year, approximately 3.9 million people die from cardiovascular diseases in Europe. The most common cause of cardiovascular diseases (myocardial infarction, strokes, etc.) and, as a consequence, the leading worldwide cause of death[6] is the atherosclerosis (other names are arteriosclerosis and hardening of the arteries). Atherosclerosis may start when certain factors cause a damage for inner layers of arteries. These factors include, for example, smoking, high amounts of certain fats and cholesterol in the blood, high blood pressure, high amounts of sugar in the blood due to insulin resistance,[11] or diabetes. Atherosclerosis is a chronic disease with asymptomatic progression for decades. Usually, atherosclerosis is a multifactorial disease that is manifested in the accumulation of protein-lipid components, collagen, and inflammatory cells on the artery wall. The last stages of atherosclerosis are characterized by a rapid decrease of blood flow velocity due to narrowing of an artery lumen. The first visible clinical signs of the disease can be elucidated only at the last stages of atherosclerosis, when the major part of the vessel's lumens is occluded.[1,2]

The diagnostic methods commonly used in medicine allow one to assess the progression of narrowing of an artery lumen that is caused by atherosclerosis. Some of these methods are listed below:

1. duplex ultrasound of blood vessels allows one to detect the volume of blood and artery damage[12];
2. magnetic resonance angiography allows one to estimate the size of atherosclerotic masses and the degree of narrowing of the vessel lumen[13];
3. computed tomography allows one to obtain layered “slices” of the artery to estimate the degree of occlusion by atherosclerotic masses. It is often used together with angiography;
4. proper angiography makes it possible to determine the volume of the blood stream in the vessel after the administration of the radiopaque substance.[14]

The progression of atherosclerotic plaque is carried out by the following stages[6,12-19]:

- First stage is the appearance of lipid spots due to the deposition of lipid-protein complexes of blood plasma in a thin layer of the inner shell of arteries.[16] Further, these spots can develop atherosclerotic plaques. The accumulation of lipoproteins on the inner shell of the artery is promoted by factors such as increased concentration of cholesterol in plasma and damaged endothelium.[17]
- Lipoprotein complexes are partially bound to the intercellular substance. Then there is oxidation, which causes local inflammation. Inflammation leads to the attachment of blood plasma leukocytes. By phagocytizing lipoproteins, macrophages are converted into xanthoma cells. This circumstance contributes to the thickening of intima and accumulation of blood plasma components, collagen, and inflammatory cells. A lipid-rich atheromatous mass appears after xanthoma cells die.[19]
- Initially, the plaque slowly grows almost without narrowing the lumen of vessel. However, over time, its growth accelerates and leads to significantly narrowing of the vessel's lumen.
- At the late stages of atherosclerosis, small ruptures causing adhesion of blood and fibrin elements appear on the surface of plaques. This process narrows the lumen even more. It is the main mechanism of thrombi formations.[10] Atherosclerosis affects vessels of different calibers, but these are mainly arteries of large and medium calibers (1–3 cm). They constitute 90–95% of the lesion.

The thrombus formation is caused by a vascular wall change, in response to which the platelets adhere to the site of injury. Further, the fibrin with the participation of platelets is formed and protein content in the growing thrombus is consolidated. At the next stage, there is a seizure and adherence of both leukocytes and erythrocytes. The final formation of the thrombus is completed by the sedimentation of plasma proteins of blood on the formed convolution and its compaction.[10] As a result of the above-described processes, the thrombus has a non-uniform layered structure. The above processes are mainly characterized by surface growth of artery wall under a thin inner layer.

1.2 | Mechanical background of growth models

The growth processes in biology can be discriminated by geometrical and mechanical features in volumetric and surface growth. There have been many attempts to mechanically and mathematically simulate the growth processes in biological materials. There are a number of in-depth reviews on mathematical and mechanical modeling aspects of growth of biological tissues.[20-27]

The main idea of volumetric growth and morphoelasticity approaches is to postulate multiplicative decomposition of deformation gradient on elastic and growth tensors. Within the framework of such techniques, several boundary value problems were stated and solved (see in-depth discusses in monograph[27]).

The ideas and concept for the mechanics of surface growth of solids are similar to some ideas of contact and impact mechanics. The problems dealt with discrete growth of a cylinder are discussed in monograph.[28] The discrete growth process can be considered as addition of some new parts to main body under boundary conditions. The problems of thermoelastoplastic discrete growth of solids under conditions of axial or central symmetry are discussed in previous studies.[29-35]

The boundary condition statement on growing surface is the fundamental problem for mechanics of surface growth. The derivations of some boundary conditions using thermodynamics principles or conservation laws can be found in a number of studies.[36-50] The principal variables of the boundary value problem for theory of surface growth for solids are the stress tensor and strain rate tensors and velocity vector. On the surface of growth, one needs to set a specific boundary condition depending on the curvature tensor of the growth surface as well as on tension and inflow rates of the incremented elements. The pathological growth of blood vessel walls can be described for some processes by model of surface growth. In the present study, we focus on the processes of surface growth for large thick-walled vessels. Some problems for an elastic thick-walled cylinder with growing surface are considered here. The condition of thickness allows us to study finite displacements of cylinder points under the condition of infinitesimal deformations. This assumption, in particular, makes it possible to solve the problem with exact boundary conditions on a moving growing surface and to investigate the behavior for characteristics of the strain-stress state depending on the pressure on the inner and outer surfaces of the cylinder.

The main purpose of the study is to obtain analytical solutions for calculating the residual stresses in the wall of a large vessel. The article presents a modification of the theory of surface growth and a solution of model problems. Comparison and generalization of the results obtained by the authors are carried out.

The second section of the article discusses the governing principles of constructing theories of surface growth. The basic concepts are determined, and time moments associated with the creation of a separate element and its entry into the main solid are introduced.

The third section deals with the basic constitutive equation of the theory of surface growth. General statements of model boundary value problems are given. The boundary value problems for thick-walled and thin-walled solids are considered separately.

Section 4 provides a solution of the Lame problem for a multilayer cylinder. The given solution is necessary for determining the stress state of the cylinder before the beginning of growth.

Section 5 discusses the general solution of the problem on the surface growth of a multilayer cylinder. The growth process begins on the inner surface of the cylinder and extends toward the luminal narrowing of the cylinder.

In Section 6, the solution obtained in the previous section is specified for the case of a single-layer cylinder growth. The results of numerical calculations are presented.

Section 7 considers an analytical solution of the problem on the growth of a two-layer cylinder. A numerical analysis of the obtained solution is carried out. The problems of approximating the obtained solution with the solution for a single-layer cylinder are discussed

In the conclusion of the article, a summary of the main results is given and possible applications of the results for modeling the pathological growth processes of vessel walls are argued.

2 | GOVERNING PRINCIPLES OF SURFACE GROWTH MECHANICS

In this paper, we use notations and concepts introduced in studies.[40,41,45,48] Description of the surface growth process involves three characteristic times: $\overset{*}{\tau}_1(\mathbf{x})$ is time when the element with the position vector $\mathbf{x}$ is created, the time $\tau_0(\mathbf{x})$ is time when a load is applied to this element, and $\overset{*}{\tau}(\mathbf{x})$ is time when the element is deposited on the growing solid. Furthermore, the star "$*$" on the top of character "**a**" has the following sense:

$$\overset{*}{a}(\mathbf{x}) = \mathbf{a}(\mathbf{x}, t)\Big|_{t=\overset{*}{\tau}(\mathbf{x})}.$$

The deposition process is determined by specifying these three times. For elastic continua, one can assume that for the surface growth process $\overset{*}{\tau}_1(\mathbf{x}) = \tau_0(\mathbf{x}) = \overset{*}{\tau}(\mathbf{x})$, i.e., the elements are deposited at the same time as they have been created $\tau_0(\mathbf{x}) = \overset{*}{\tau}(\mathbf{x})$. In some cases, the time $\overset{*}{\tau}_1(\mathbf{x})$ can differs on deposition or loading times. Moreover, the deformation can be accumulated as soon as element is created and added to the main solid, i.e., $\overset{*}{\tau}_1(\mathbf{x}) = \tau_0(\mathbf{x}) \neq \overset{*}{\tau}(\mathbf{x})$.

We suggest an approach to modeling the surface growth processes in solids on the basis of the following postulates[48]:

- The growth process of a solid is modeled by the motion of its boundary due to the influx of new material to the growing surface.
- The stress rate tensor, strain rate tensor (or the stretch rate tensor), and the velocity vector are the main variables in the system of equations describing the growth process.
- We use special kinematic and quasistatic conditions on the moving boundary (growing or deposition surface) that determine the conservation law for a growing solid composition and specific contact interaction between 3D solid and 2D deposited surfaces.

To simplify the problem, the non-inertial cases of boundary value problems with zero volumetric force is considered. The material description of the mechanics of surface growth processes that differs from known approaches in continuum mechanics is proposed. Existing approaches to material description (see, e.g., Zhilin et al.[51]) use stress and strain tensors as well as displacement vector as basic variables of boundary value problems. We use stress rates tensor, stretch tensor, and velocity vector.

3 | THE GOVERNING EQUATIONS OF SURFACE GROWTH THEORY

The solution of each specific problem for a growing solid is an independent and complicated problem.[45,48] Within the framework of the mechanics of growing solids, an essential feature of the formulation of boundary value problems is the statement of boundary conditions on the surface between main body and growing part.[38,40-42] In this section, we consider several variants of the boundary value problems. Constitutive equations in mechanics of growing solids are usually presented in terms of velocities of the physical fields. The parameters of stress-strain state can be recovered via its velocities by following formulas in operator form

$$\boldsymbol{\sigma}(\mathbf{x}, t) = \overset{*}{\boldsymbol{\sigma}}(\mathbf{x}) + \int\limits_{\overset{*}{\tau}(\mathbf{x})}^{t} \partial_t \boldsymbol{\sigma}(\mathbf{x}, t')\, dt', \qquad \mathbf{u}(\mathbf{x}, t) = \overset{*}{u}(\mathbf{x}) + \int\limits_{\overset{*}{\tau}(\mathbf{x})}^{t} \mathbf{v}(\mathbf{x}, t')\, dt', \tag{1}$$

and in coordinate form

$$\sigma^{ij}(x^k, t) = \overset{*}{\sigma}{}^{ij}(x^k) + \int\limits_{\overset{*}{\tau}(x^k)}^{t} \partial_t \sigma^{ij}(x^k, t')\, dt', \qquad u^i(x^k, t) = \overset{*}{u}{}^i(x^k) + \int\limits_{\overset{*}{\tau}(x^k)}^{t} v^i(x^k, t')\, dt'. \tag{2}$$

Herein, $\boldsymbol{\sigma} = \sigma^{ij}$ is the Cauchy stress tensor, $\overset{*}{\boldsymbol{\sigma}}(\mathbf{x}) = \boldsymbol{\sigma}|_{t=\overset{*}{\tau}(\mathbf{x})}$; $\mathbf{u} = u^i$ is the displacement vector, $\overset{*}{u}(\mathbf{x}) = u\Big|_{t=\overset{*}{\tau}(\mathbf{x})}$; $\mathbf{v}$ is the velocity vector; and ∂_t denotes the derivative on time. The present equations (2) are the simple integrating rule of primitives. We note that all necessary initial conditions for values in (1) and (2) as well as load changes with time as the parts and structures grow are given.

3.1 | The general nonlinear boundary value problem

In the current subsection, we consider the nonlinear theory of surface growth process for a hyperelastic continuum. In terms of velocities, the equilibrium equation can be derived in following operator form:

$$\boldsymbol{\nabla} \cdot (\partial_t \boldsymbol{\sigma}) = \mathbf{0}, \tag{3}$$

Boundary conditions on a non-growing part of the surface are

$$\mathbf{x} \in \Sigma_1 \ : \ \mathbf{n} \cdot \partial_t \boldsymbol{\sigma} = \partial_t \mathbf{p}_0, \qquad \mathbf{x} \in \Sigma_2 \ : \ \mathbf{v} = \partial_t \mathbf{u}_0. \tag{4}$$

Condition on a growing surface that is obtained from the solution of contact interaction problem between 3D solid and 2D surface is as follows:

$$\mathbf{x} \in \overset{*}{\Sigma}(t) \ : \ \ \mathbf{n} \cdot \partial_t \boldsymbol{\sigma} = -s_n (\mathcal{T}_s \ : \ \mathbf{L})\, \mathbf{n}, \ s_n = \mathbf{n} \cdot \mathbf{v}. \tag{5}$$

Kinematic boundary condition on a growing surface (the conservation law for a growing solid composition) is

$$\mathbf{x} \in \overset{*}{\Sigma}(t) \ : \ \ \mathbf{v} = \mathbf{v}_{\text{def}} + \mathbf{v}_{\text{gr}}. \tag{6}$$

Relation between the strain rates and velocities is

$$\mathbf{D} = \frac{1}{2}(\boldsymbol{\nabla} \otimes \mathbf{v} + \mathbf{v} \otimes \boldsymbol{\nabla}), \tag{7}$$

and the constitutive equation has the form

$$\partial_t \boldsymbol{\sigma} = 2\mathcal{F}_t(\mathbf{D}, \mathbf{v}). \tag{8}$$

The equation of the propagating growing surface $\overset{*}{\Sigma}(t)$ for a growing solid can be assumed in the implicit form as follows:

$$t = \overset{*}{\tau}(\mathbf{x}), \tag{9}$$

where $\boldsymbol{\nabla}$ is the Hamilton (nabla) operator, $\mathbf{p}_0$ is the given traction vector, $\mathbf{u}_0$ are the given displacements vectors, $\mathbf{n}$ is the unit vector of normal to the surface of solid, $\mathcal{T}_s$ is the 2D tensor of the given elastic surface tension, $\mathbf{L}$ is the 2D tensor of the surface curvature, $\mathbf{D}$ is the strain rate tensor, $\mathbf{v}_{\text{def}}$ is the velocity of the boundary surface due to deformation of a solid, and $\mathbf{v}_{\text{gr}} = -\mathbf{v}_{\text{dep}}$ is the prescribed velocity of growth that is opposite to the velocity of deposition of a new material to the growing surface.

Equations (3)–(9) supplemented by the recovering formulae (1) state the boundary value problem for a surface growing solid in a nonlinear case. It should be noted that the boundary value problem for a growing solid contains following set of controlled values, namely, loads, stresses on the propagating growing surface, and velocity of deposition.

3.2 | Theory of surface growth for thin-walled solids

Term «thin-walled parts» means such solids, which are subjected to large displacements and small strains during the growing and deforming processes. In this case, we can use linear constitutive equations (Hooke's law) while boundary conditions are still nonlinear and growing surface is unknown. In this case, we obtain the boundary value problem like in Section 3.1 in the operator form

$$\begin{aligned}
&\boldsymbol{\nabla} \cdot (\partial_t \boldsymbol{\sigma}) = \mathbf{0}, \ \partial_t \boldsymbol{\sigma} = 2\mu \mathbf{D} + \lambda \operatorname{tr}(\mathbf{D})\mathbf{I}, \ \mathbf{D} = \frac{1}{2}(\boldsymbol{\nabla} \otimes \mathbf{v} + \mathbf{v} \otimes \boldsymbol{\nabla}), \ \mathbf{v} = \mathbf{v}_{\text{def}} + \mathbf{v}_{\text{gr}}, \\
&\mathbf{x} \in \Sigma_1 \ : \ \mathbf{n} \cdot \partial_t \boldsymbol{\sigma} = \partial_t \mathbf{p}_0, \qquad \mathbf{x} \in \Sigma_2 \ : \ \mathbf{v} = \partial_t \mathbf{u}_0, \\
&\mathbf{x} \in \overset{*}{\Sigma}(t) \ : \ \mathbf{n} \cdot \partial_t \boldsymbol{\sigma} = -s_n (\mathcal{T}_s \ : \ \mathbf{L})\, \mathbf{n}, \ s_n = \mathbf{n} \cdot \mathbf{v}, \ t = \overset{*}{\tau}(\mathbf{x}).
\end{aligned} \tag{10}$$

where λ, μ are the Lamé parameters. Note that the velocity of propagating growing surface consists of the velocity occurred due to deposition of a new material and velocity appearing due to deformation of solids.

3.3 | Theory of surface growth for thick-walled parts

Consider the theory of mechanical behavior of growing solids for infinitesimal deformations. It is quite clear that one deals with thick-walled structures, the deformation of which for classical structural materials in the growing processes and loading is infinitesimal. In this case, the velocity of growing surface that appears due to deformation of solids $\mathbf{v}_{\text{def}}$ can be eliminated, because this term is infinitesimal in comparison with the propagation velocity of growing surface. In this case, we can simplify the boundary value problem (3.2) as follows

$$\begin{aligned}
&\boldsymbol{\nabla}\cdot(\partial_t\boldsymbol{\sigma})=\mathbf{0},\ \partial_t\boldsymbol{\sigma}=2\mu\mathbf{D}+\lambda\text{tr}(\mathbf{D})\mathbf{I},\ \mathbf{D}=\frac{1}{2}(\boldsymbol{\nabla}\otimes\mathbf{v}+\mathbf{v}\otimes\boldsymbol{\nabla}),\ \mathbf{v}=\mathbf{v}_{\text{gr}},\\
&\mathbf{x}\in\Sigma_1\ :\ \mathbf{n}\cdot\partial_t\boldsymbol{\sigma}=\partial_t\mathbf{p}_0,\qquad \mathbf{x}\in\Sigma_2\ :\ \mathbf{v}=\partial_t\mathbf{u}_0,\\
&\mathbf{x}\in\overset{*}{\Sigma}(t)\ :\ \mathbf{n}\cdot\partial_t\boldsymbol{\sigma}=-s_n(\mathcal{T}_s\ :\ \mathbf{L})\,\mathbf{n},\ s_n=\mathbf{n}\cdot\mathbf{v},\ t=\overset{*}{\tau}(\mathbf{x}).
\end{aligned}\tag{11}$$

Equation (11) forms the general boundary value problem for thick-walled solids. This boundary value problem is mathematically identical to the boundary value problem of the theory of elasticity for small deformations, and the most adequate results are obtained within the framework of this version of the theory (see, e.g., previous works[45-48]).

Both simplified theories discussed in Sections 3.2 and 3.3 for thin (10) and thick (11) walled growing solids give adequate mathematical models of growing processes for different applications. Nevertheless, the development of the general nonlinear theory is very important especially from the point of view of new constitutive equation for material description of a continuum with microstructure.

4 | GROWTH OF ELASTIC THICK-WALLED MULTILAYER CYLINDER

4.1 | Elastic equilibrium in cylindrical coordinate frame: Lamé problem

The problem considered below has been solved within the framework of the boundary value problem discussed in Section 3.3. In order to simplify the solution, the condition of axial symmetry in cylindrical coordinates and the condition of the plane deformed state (an infinitely long hollow cylinder) are used. The equilibrium equation (3) under cylindrical symmetry condition can be represented as follows:

$$\frac{\partial\sigma_{rr}}{\partial r}+\frac{\sigma_{rr}-\sigma_{\varphi\varphi}}{r}=0,\tag{12}$$

where σ_{rr} is the radial stress and $\sigma_{\varphi\varphi}$ is the circumferential one. For the radial strain tensor component e_{rr} and the circumferential one $e_{\varphi\varphi}$, the following equations take place:

$$e_{rr}=\frac{\partial u_r}{\partial r},\ e_{\varphi\varphi}=\frac{u_r}{r},\tag{13}$$

wherein u_r is the radial displacement.

Consider a multilayer elastic cylinder consisting of different elastic materials. Hooke's law for a cylinder can be manifested in the following form:

$$\sigma_{rr}^{(i)}=(\lambda_i+2\mu_i)e_{rr}^{(i)}+\lambda_i e_{\varphi\varphi}^{(i)},\ \sigma_{\varphi\varphi}^{(i)}=(\lambda_i+2\mu_i)e_{\varphi\varphi}^{(i)}+\lambda_i e_{rr}^{(i)},\tag{14}$$

where $(i=1\ \dots\ n)$ is the layer number, λ_i, μ_i are Lamé material constants for ith layer. The elastic properties of Hooke's material are determined by two coefficients: Young's modulus E and Poisson's ratio ν. Note that dimensionless boundary value problem can provide the solution for a hypothetical material in simple form that is independent of the material constants and can elucidate the quality features of the solution. In the present article, for the dimensionless numerical simulation, the values of Young's modules for each layer are different and reduced to dimensionless parameter by $\alpha_i=E_i/E_0$. Hereinafter, the values measured in Pascals (elastic modulus and stresses) are divided by the value of Young's modulus of the growing layer. Poisson's ratio varies within the range $0.2 < \nu_i < 0.4$. Expressions for the Lamé parameters imply a set of different values λ_i and μ_i, which depend on the choice of dimensionless parameters ν_i and α_i:

$$\lambda_i = \frac{\alpha_i \nu_i}{(1+\nu_i)(1-2\nu_i)}, \ \mu_i = \frac{\alpha_i}{2(1+\nu_i)}. \tag{15}$$

The general solution of the equation of equilibrium (12) under conditions of constitutive equations (14) and (13) can be obtained as follows:

$$\sigma_{rr}^{(i)} = A_i + \frac{B_i}{r^2}, \ \sigma_{\varphi\varphi}^{(i)} = A_i - \frac{B_i}{r^2}, \ \sigma_{zz}^{(i)} = \frac{\lambda_i A_i}{\gamma_i}, \ u_r^{(i)} = \frac{A_i r}{2\gamma_i} - \frac{B_i}{2\mu_i r}, \ \gamma_i = \lambda_i + \mu_i. \tag{16}$$

Here, A_i, B_i are unknown integrating constants determined from the boundary conditions of the problem.

The solution of specific problem defined by Equation (16) is need to be supplemented by the specific boundary conditions. Consider the multilayer cylinder with size of each layer $R_{(i-1)} < r < R_i$ $(i = 1 \ldots n)$. Then the inner surface of the cylinder $r = R_0$ corresponds to the inner surface of the first inner layer, the outer surface of the cylinder $r = R_n$ corresponds to the outer surface of the last outer layer. The surfaces $r = R_i$ $(i = 1 \ldots (n-1))$ are the contact surfaces between the layers. Average pressures act on the inner and outer surfaces:

$$\sigma_{rr}^{(1)}(R_0) = p_0, \ \sigma_{rr}^{(n)}(R_n) = p_n. \tag{17}$$

On the contact surfaces $r = R_i$ $(i = 1 \ldots (n-1))$, the conditions for continuity of radial stress and radial displacement have the form

$$\sigma_{rr}^{(i)}(R_i) = \sigma_{rr}^{(i+1)}(R_i), \ u_r^{(i)}(R_i) = u_r^{(i+1)}(R_i) \ (i = 1 \ldots (n-1)). \tag{18}$$

Integrating constants A_i, B_i are found from the solution of a system of linear equations (17) and (18) taking account of Lamé problem solution (16). In following sections, we consider specific boundary value problems on deformation of a concentrically growing multilayer and single-layer cylinder.

5 | BOUNDARY VALUE PROBLEM FOR A SURFACE GROWTH OF A MULTILAYER THICK-WALLED CYLINDER

The predefined stress-strain state of the multilayer cylinder is described by the solution (16). Assume that at time $t = t_0$, a new material is added on the inner surface of the cylinder (appearing growing layer $i = 0$). The law of motion of propagating growing surface in the direction of the axis of symmetry can be chosen on the following simple form:

$$R(t) = \sqrt{R_0^2 - mt}, \tag{19}$$

where $m > 0$ is growing volume per unit of time. It is need to account the additional inequality ($R_0^2 \geq mt$) for elimination of negative values under radical in (19). The stress-strain state of a cylinder depends on the rate of growth. The boundary value problem in virtue of (11) and taking into account the axial symmetry condition can be derived in the form

$$\partial_t \sigma_{rr}^{(i)} = X_i(t) + \frac{Y_i(t)}{r^2}, \ \partial_t \sigma_{\varphi\varphi}^{(i)} = X_i(t) - \frac{Y_i(t)}{r^2}, \ \partial_t \sigma_{zz}^{(i)} = \frac{\lambda_i X_i(t)}{\gamma_i}, \ \partial_t u_i = \frac{X_i(t) r}{2\gamma_i} - \frac{Y_i(t)}{2\mu_i r}. \tag{20}$$

where $Y_i(t)$, $X_i(t)$ are the unknown time dependent functions derived from boundary conditions and i takes the values from 0 to n as follows:

$$\begin{gathered} \partial_t \sigma_{rr}^{(0)}(R(t)) = \frac{s_n(t)\tau(t)}{R(t)}, \ s_n(t) = \partial_t R(t) = -0.5m(R_0^2 - mt)^{-1/2}, \\ \partial_t \sigma_{rr}^{(i)}(R_i) = \partial_t \sigma_{rr}^{(i+1)}(R_i), \ \partial_t \sigma_{rr}^{(n)}(R_n) = 0, \ \partial_t u_r^{(i)}(R_i) = \partial_t u_r^{(i+1)}(R_i), \end{gathered} \tag{21}$$

where $\tau(t)$ is a tension on the growing surface given from the experiment data for each growth process.

We can obtain solutions for stresses and displacements in each layer $i = 1 \ldots n$ for given time $t > t_0$ by integrating solutions (20) in time due to the formulae of restoration (2) in following form:

$$\begin{aligned}
&\sigma_{rr}^{(i)} = A_i + \frac{B_i}{r^2} + \int_{t_0}^{t} \left(X_i(s) + \frac{Y_i(s)}{r^2} \right) ds, \ \sigma_{\varphi\varphi}^{(i)} = A_i - \frac{B_i}{r^2} + \int_{t_0}^{t} \left(X_i(s) - \frac{Y_i(s)}{r^2} \right) ds, \\
&\sigma_{zz}^{(i)} = \frac{\lambda_i}{\gamma_i} \left| A_i + \int_{t_0}^{t} X_i(s) ds \right|, \ u_r^{(i)} = \frac{A_i r}{2\gamma_i} - \frac{B_i}{2\mu_i r} + \left| \int_{t_0}^{t} \frac{X_i(s) r}{2\gamma_i} - \frac{Y_i(s)}{2\mu_i r} \right| ds.
\end{aligned} \tag{22}$$

The solutions for the growing layer can be presented by formulae

$$\begin{aligned}
&\sigma_{rr}^{(0)} = p_0 + \int_{t_0}^{t} \left(X_0(s) + \frac{Y_0(s)}{r^2} \right) ds, \ \sigma_{\varphi\varphi}^{(0)} = A_1 - \frac{B_1}{R_0^2} + \int_{t_0}^{t} \left(X_0(s) - \frac{Y_0(s)}{r^2} \right) ds, \\
&\sigma_{zz}^{(0)} = \frac{\lambda_1 A_1}{\gamma_1} + \frac{\lambda_0}{\gamma_0} \int_{t_0}^{t} X_0(s) ds, \ u_r^{(0)} = \frac{A_1 R_0}{2\gamma_1} - \frac{B_1}{2\mu_1 R_0} + \left| \int_{t_0}^{t} \frac{X_0(s) r}{2\gamma_0} - \frac{Y_0(s)}{2\mu_0 r} \right| ds.
\end{aligned} \tag{23}$$

Using solutions (22) and (23), we will analyze the influence of Lamé parameters on the formation of the stress-strain state of a material under growth conditions in different specific cases in the following sections.

6 | SINGLE-LAYER GROWING CYLINDER

In this section, we consider a single-layer cylinder with the material parameters λ_1, μ_1. Cylinder has internal and external radii $R_0 < r < R_1$. Growth process is begun at time $t = t_0$ with the parameters λ_0, μ_0. Constants A_1, B_1, X_1, Y_1, X_0, Y_0 are computed using the system of boundary conditions (17), (18), (21) in the following form:

$$\begin{aligned}
&X_0 = -\Psi^{-1}\gamma_0 \left[(\mu_0 - \mu_1)\gamma_1 R_1^2 + \mu_1(\gamma_1 + \mu_0) R_0^2 \right], \ A_1 = -(R_1^2 - R_0^2)^{-1}(p_1 R_0^2 + p_2 R_1^2), \\
&Y_0 = \Psi^{-1}\mu_0 \left[\mu_1(\gamma_0 - \gamma_1) R_0^2 + \gamma_1(\gamma_0 + \mu_1) R_1^2 \right] R_0^2, \ B_1 = (R_1^2 - R_0^2)^{-1}(p_1 + p_2) R_0^2 R_1^2, \\
&X_1 = -\Psi^{-1}(\lambda_0 + 2\mu_0)\mu_1\gamma_1 R_0^2, \ Y_1 = \Psi^{-1}(\lambda_0 + 2\mu_0)\mu_1\gamma_1 R_0^2 R_1^2, \\
&\Psi = \left\{ \mu R_0^2 \left[\mu_1 R_0^2(\gamma_0 - \gamma_1) + \gamma_1(\gamma_0 + \mu_1) R_1^2 \right] - \gamma_0 R^2(t) \left[(\mu_0 - \mu_1)\gamma_1 R_1^2 + \mu_1(\gamma_1 + \mu_0) R_0^2 \right] \right\} \cdot [R_0(t)\tau(t)s(t)]^{-1}.
\end{aligned} \tag{24}$$

The results of calculations of stress fields at different moments of time for a given set of material constants are presented in Figures 1–7. The following dimensionless material constants have been used in the following calculations: $\nu = 0.3$, $p_0 = 0.001$, $p_n = 0.0001$, $\tau = 0.0055$, $m = 0.05$.

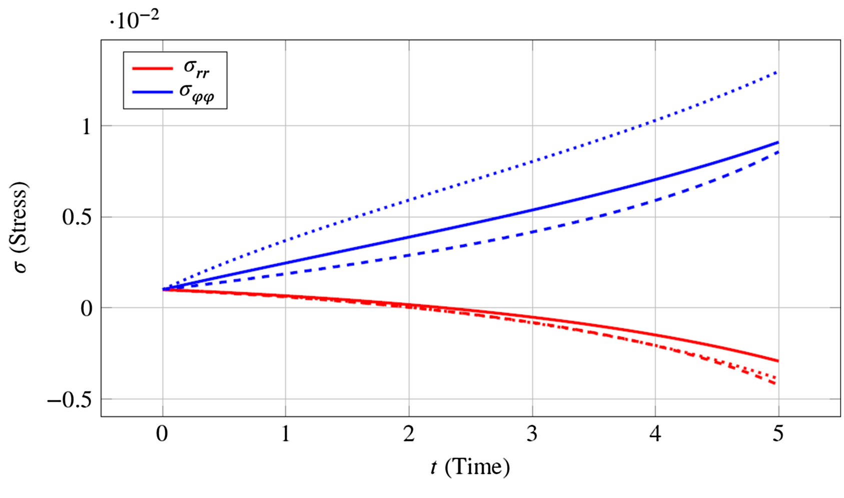

FIGURE 1 Radial σ_{rr} (red lines) and circumferential $\sigma_{\varphi\varphi}$ (blue lines) stresses on the free growing surface for $\alpha_1 = 1$ (solid line), $\alpha_1 = 2$ (dashed lines), $\alpha_1 = 0.5$ (dotted lines)

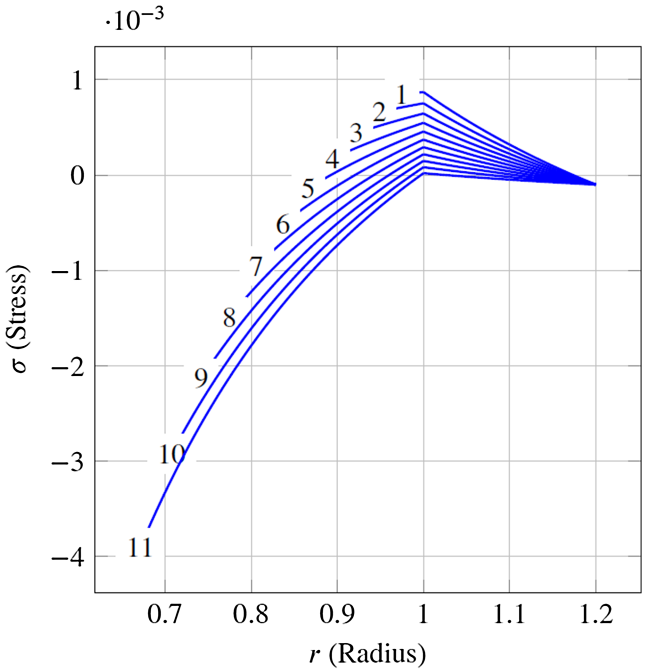

FIGURE 2 σ_{rr} at the different times, $\alpha_1 = 1$, $R_1/R_0 = 1.2$

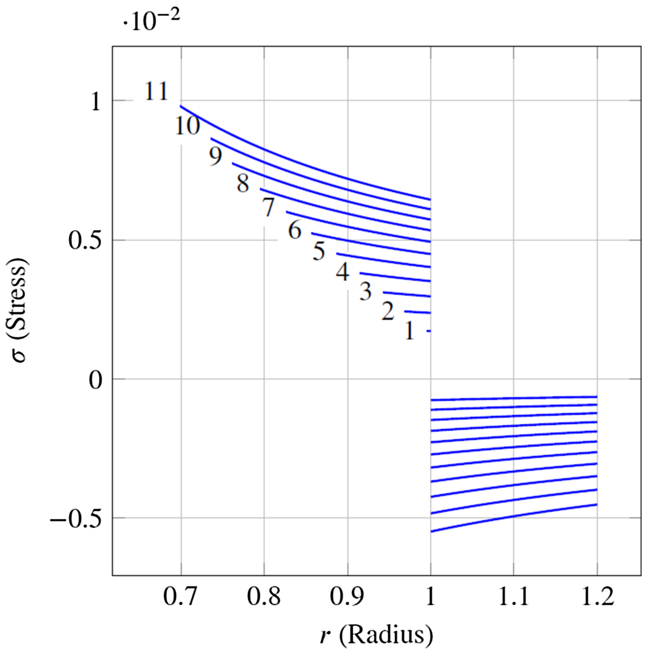

FIGURE 3 $\sigma_{\varphi\varphi}$ at the different times, $\alpha_1 = 1$, $R_1/R_0 = 1.2$

The equality of the fields of radial and circumferential stresses on the growth surface at the initial moment of time is due to the fulfillment of the equilibrium equation at the moment of attachment of the growing layer. It follows from the plot that a two-fold increase in Young's modulus reduces the absolute value of the radial and circumferential stress on the free growing surface by 50%. A decrease in Young's modulus in the material of the cylinder increases the stresses of the growing layer on the growth surface by 50%. This difference is weakly dependent on time of growth and can be considered as a constant.

FIGURE 4 σ_{rr} at the different times, $\alpha_1 = 2, R_1/R_0 = 1.2$

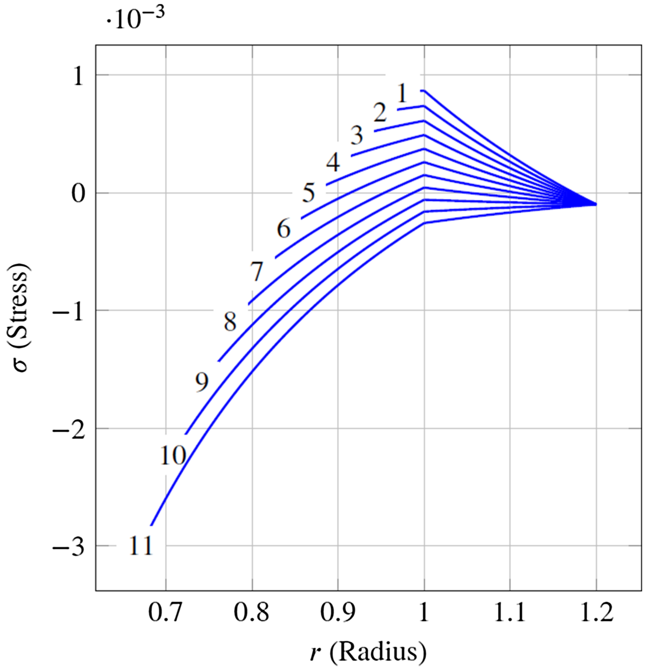

FIGURE 5 $\sigma_{\varphi\varphi}$ at the different times, $\alpha_1 = 2, R_1/R_0 = 1.2$

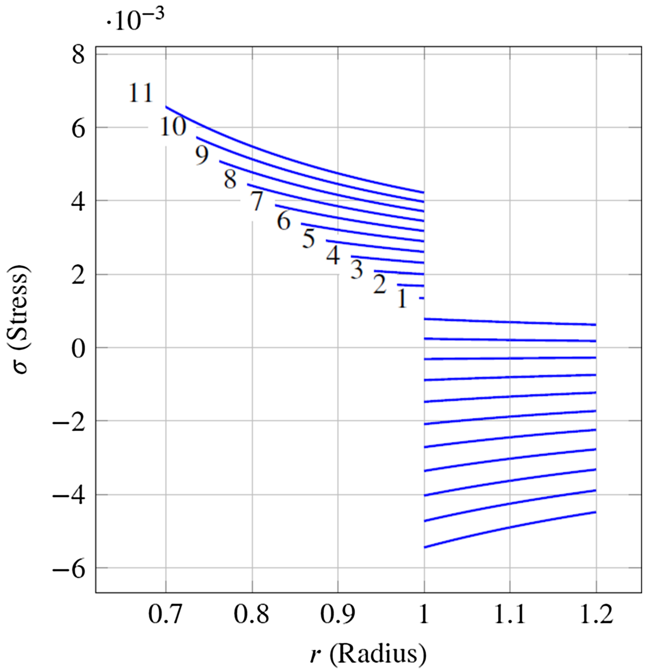

In Figure 8, the change in the magnitude of the circumferential stress on the growth surface is presented depending on the choice of Young's modulus for the cylinder. Based on the data obtained from the numerical simulations of boundary value problems, one can conclude that the stresses on growing surface have the similar time plots. The following formula allows us to approximate results by a simple scaling equation

$$\sigma_{ij}(R(t), \alpha_1) = \frac{\sigma_{ij}(R(t), 1)}{\sqrt{(\alpha_1)}}. \tag{25}$$

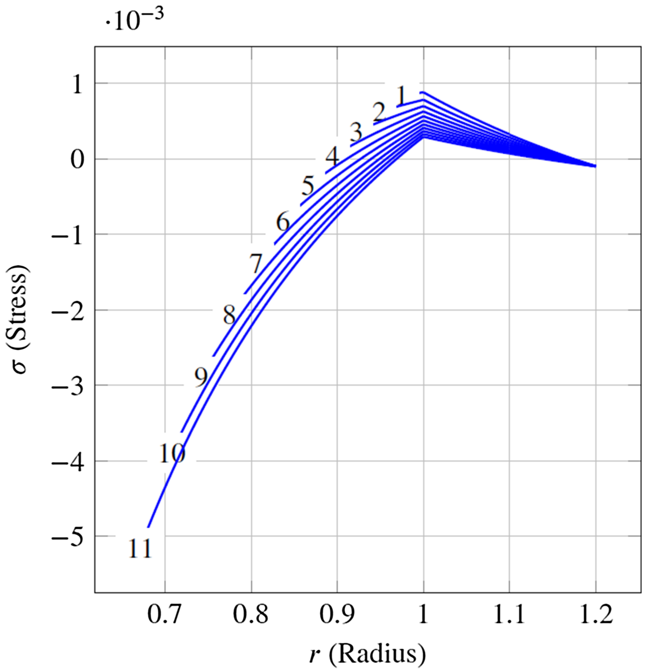

FIGURE 6 σ_{rr} at the different times, $\alpha_1 = 0.5$, $R_1/R_0 = 1.2$

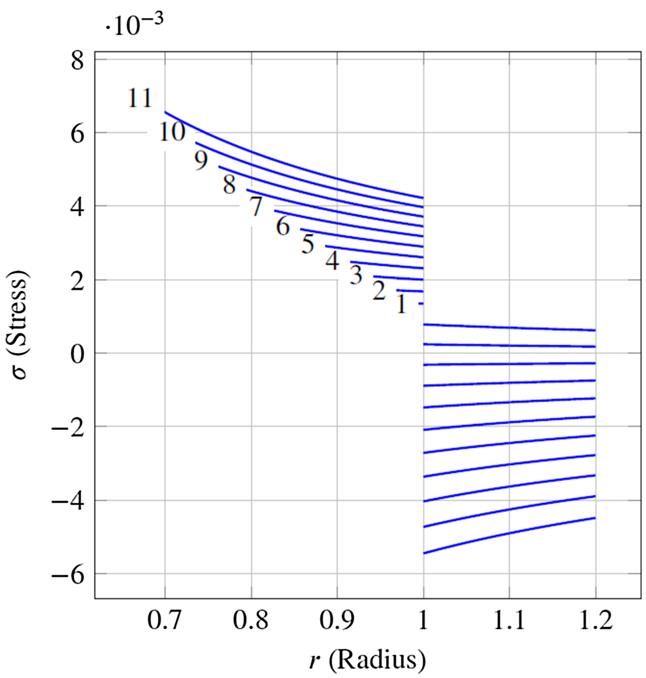

FIGURE 7 $\sigma_{\varphi\varphi}$ at the different times, $\alpha_1 = 0.5$, $R_1/R_0 = 1.2$

It follows from Figure 8 that the best degree of approximation is for $\alpha_1 < 1$, which corresponds to the ratio of parameters for the material of blood vessels. Note that if the constant α_1 retains its value and the value of Young's modulus of the growing layer is different for a particular calculation, then the stress values are directly proportional to the value of Young's modulus of the growing layer. The maximum level of stresses on the contact surface depends on the boundary conditions and the value of the inner radius of the layer (since the pressure on the inner surface is much higher than the pressure on the outer one). It has been found that the ratio (25) approximates the dependence of stresses on α_1 regardless of the choice R_0 and with the same degree of accuracy.

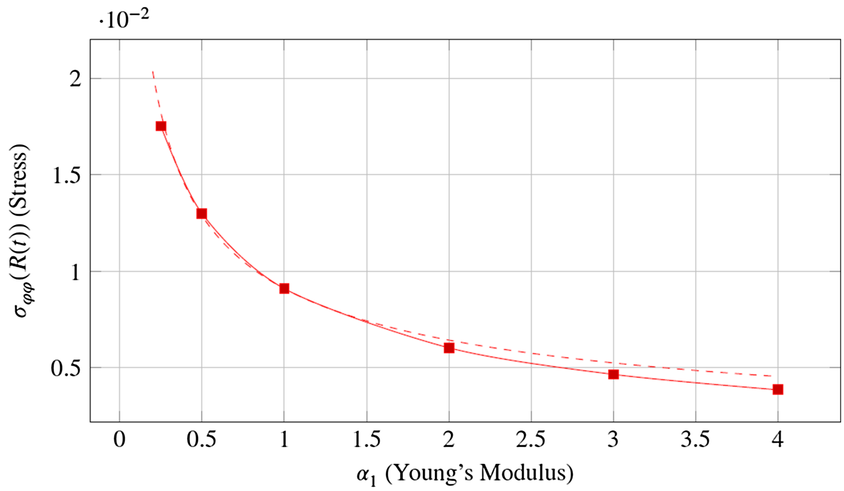

FIGURE 8 The dependence of the level of circumferential stress on the growth surface of the magnitude of Young's modulus of a single-layer cylinder. The markers indicate the calculation data, the dotted line indicates the approximation dependence (25)

7 | TWO-LAYERED GROWING CYLINDER

In this section, we consider the problem of computation of the stress-strain state of a growing two-layer cylinder on its inner surface. The system of equations describing the boundary conditions takes the form

$$\partial_t \sigma^0_{rr}(R_0) = \partial_t \sigma^1_{rr}(R_0),\ \ \partial_t u^0_r(R_0) = \partial_t u^1_r(R_0),\ \ \partial_t \sigma^1_{rr}(R_1) = \partial_t \sigma^2_{rr}(R_1),\ \ \partial_t u^1_r(R_1) = \partial_t u^2_r(R_1). \tag{26}$$

The unknown functions are calculated using the general solution (22) and (23) supplemented by the conditions (26) in following form:

$$\begin{aligned}
X_0 =& \gamma_0 \Psi_1^{-1}[(\gamma_1-\gamma_2)(\mu_0-\mu_1)\mu_2 R_1^4 + \gamma_2(\mu_1-\mu_2)R_0^2R_2^2(\gamma_1+\mu_0)] \\
&+ R_1^2[\mu_2 R_0^2(\gamma_1+\mu_0)(\gamma_2+\mu_1) + \gamma_2(\mu_0-\mu_1)R_2^2(\gamma_1+\mu_2)], \\
Y_0 =& \mu_0 R_0^2 \Psi_1^{-1}[(\gamma_1-\gamma_2)\mu_2 R_1^4(\gamma_0+\mu_1) + (\gamma_0-\gamma_1)\gamma_2(\mu_1-\mu_2)R_0^2R_2^2] \\
&+ R_1^2[(\gamma_0-\gamma_1)\mu_2 R_0^2(\gamma_2+\mu_1) + \gamma_2 R_2^2(\gamma_0+\mu_1)(\gamma_1+\mu_2)], \\
X_1 =& \gamma_1 \Psi_1^{-1} R_0^2(\gamma_1+\mu_1)[\mu_2 R_1^2(\gamma_2+\mu_1) + \gamma_2(\mu_1-\mu_2)R_2^2], \\
Y_1 =& \Psi_1^{-1}\mu_1 R_0^2 R_1^2(\gamma_1+\mu_1)[(\gamma_1-\gamma_2)\mu_2 R_1^2 + \gamma_2 R_2^2(\gamma_1+\mu_2)], \\
X_2 =& \gamma_2\mu_2\Psi_1^{-1}R_0^2R_1^2(\gamma_0+\mu_0)(\gamma_1+\mu_1),\ \ Y_2 = \Psi_1^{-1}\gamma_2\mu_2 R_0^2R_1^2R_2^2(\gamma_0+\mu_0)(\gamma_1+\mu_1), \\
A_1 =& \frac{p_0R_0^2 + p_nR_1^2}{R_0^2-R_1^2},\ \ B_1 = -\frac{(p_0+p_n)R_0^2R_1^2}{R_0^2-R_1^2}, \\
A_2 =& \frac{\gamma_2\{\mu_2p_0R_0^2(\gamma_1+\mu_1) + p_n[\gamma_1(\mu_2-\mu_1)R_0^2 + \mu_1R_1^2(\gamma_1+\mu_2)]\}}{\gamma_1\mu_1(R_0^2-R_1^2)(\gamma_2+\mu_2)}, \\
B_2 =& \frac{\mu_2R_1^2\{\gamma_2p_0R_0^2(\gamma_1+\mu_1) + p_n[\gamma_1R_0^2(\gamma_2+\mu_1) + (\gamma_2-\gamma_1)\mu_1R_1^2]\}}{\gamma_1\mu_1(R_1^2-R_0^2)(\gamma_2+\mu_2)}, \\
\Psi_1 =& \big(\gamma_0R(t)^2\{(\gamma_1-\gamma_2)(\mu_0-\mu_1)\mu_2R_1^4 + R_1^2[\mu_2R_0^2(\gamma_1+\mu_0)(\gamma_2+\mu_1) \\
&+ \gamma_2(\mu_0-\mu_1)R_2^2(\gamma_1+\mu_2)] + \gamma_2(\mu_1-\mu_2)R_0^2R_2^2(\gamma_1+\mu_0)\} - \\
&- \mu_0R_0^2\{(\gamma_1-\gamma_2)\mu_2R_1^4(\gamma_0+\mu_1) + R_1^2[(\gamma_0-\gamma_1)\mu_2R_0^2(\gamma_2+\mu_1) \\
&+ \gamma_2R_2^2(\gamma_0+\mu_1)(\gamma_1+\mu_2)] + (\gamma_0-\gamma_1)\gamma_2(\mu_1-\mu_2)R_0^2R_2^2\}\big)\,(R(t)s(t)\tau(t))^{-1}.
\end{aligned}$$

The typical stresses for given parameters are shown on Figures 9–11. To eliminate the influence of the geometric parameters of the cylinder, we take the values of the inner radius of the inner layer and the outer radius of the outer layer to be equal to the inner and outer radius of the single-layer cylinder from the previous section. The radius of the contact surface between the layers is given in the following form: $R_1 = (R_0 + R_2)/2$.

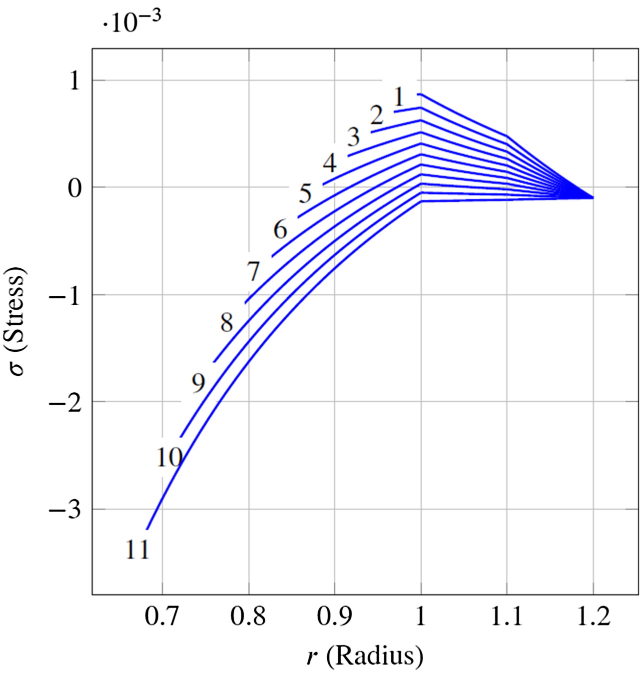

FIGURE 9 σ_{rr} at the different times, $\alpha_1 = 1$, $\alpha_2 = 2$, $R_1/R_0 = 1.1$, $R_2/R_0 = 1.2$

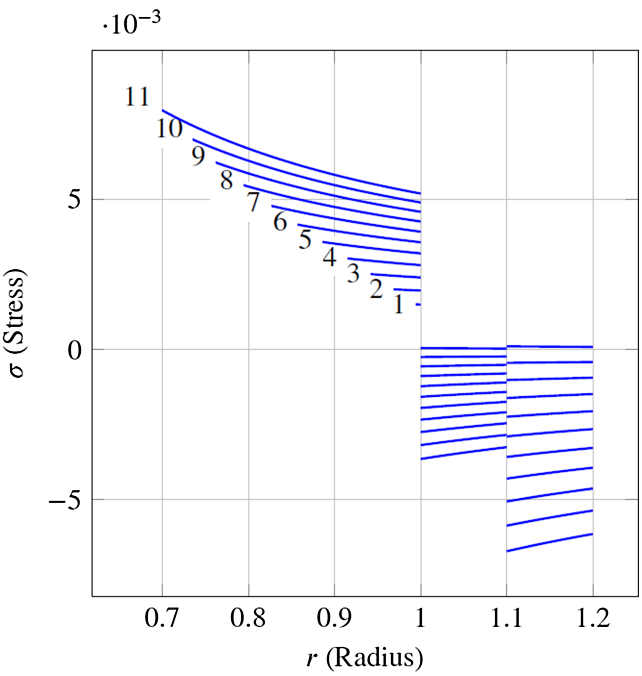

FIGURE 10 $\sigma_{\varphi\varphi}$ at the different times, $\alpha_1 = 1$, $\alpha_2 = 2$, $R_1/R_0 = 1.1$, $R_2/R_0 = 1.2$

Based on the analysis of numerical solutions of a two-layer cylinder, it has been shown that the parameters of both layers can be chosen so that the stress-strain state of the composite material corresponds to the stress-strain state of one layer with a given value of α_1^*. This approach allows us to estimate the effect of a change of Young's modulus in each material depending on the position of the contact boundary between the layers. The ratio, which allows replacing the composite material with a single-layer analog (while maintaining the values of the inner and outer surfaces), can be assumed in the following form

$$2\alpha_1^* = \alpha_1 \frac{R_2}{R_1} + \alpha_2 \frac{R_0}{R_1}. \tag{27}$$

The maximum difference between the solution for two-layer cylinder and solution for single-layer cylinder with elastic modulus α_1^* that has been calculated using equation (27) is 1.6%. As a result, we have simplified the analysis of the influence of the parameters of each layer and passed to the dependencies presented in previous paragraph.

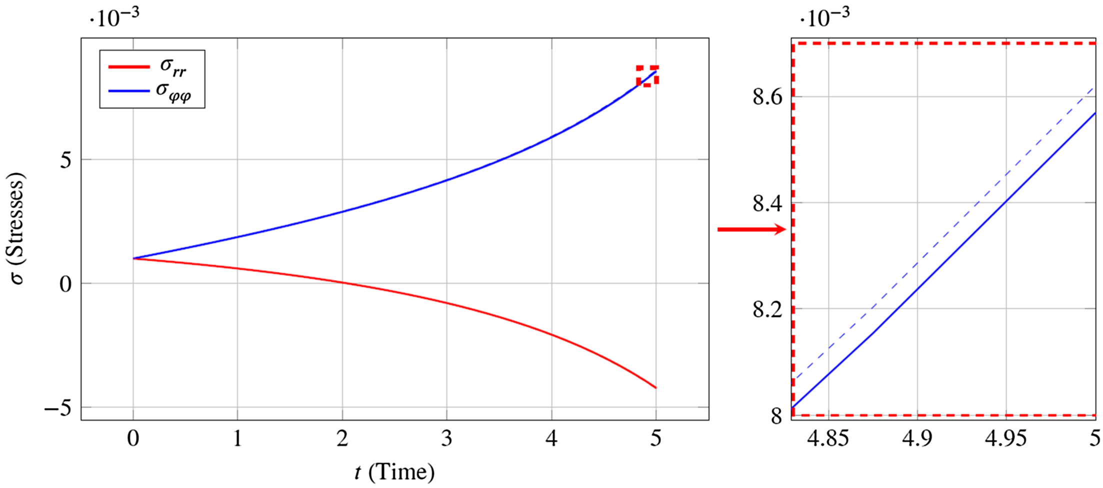

FIGURE 11 σ_{rr} and $\sigma_{\varphi\varphi}$ on the free growing surface for one-layer cylinder ($\alpha_1^* = 2$) and two-layer cylinder ($\alpha_1 = 1$, $\alpha_2 = 3.2$, dashed lines)

8 | CONCLUSIONS

Some fundamental principles for mechanics of surface growth have been formulated and discussed. The set of boundary value problems on the surface growth processes have been solved. The stress-strain state of the growing material, on the inner surface of which the process of continuous growth is performed, has been investigated. The features of the formation of the stress-strain state with different material parameters for cases of single- and two-layer cylinders have been discussed. Assessment of the influence of Young's modulus on the magnitude of the maximum stresses on the growing surface that determines the allowable limit of stable growth is performed. For a composite biomaterial, the possibility of replacing the original problem with a similar one with a single layer, the parameters of which can influence the residual stresses on a growing surface in the same way, has been estimated. Stress distributions have been constructed for various material parameters. As a result, we have estimated the value of stresses on the contact surface between the growing layer and the main solid layer.

The obtained analytical solution of the problems on the luminal narrowing of the vascular wall allows us to estimate the stress concentration on the inner wall of the vessel. The concentration of residual stresses that occurs during growth results in rupture of the inner vascular membrane, which leads to vessel thrombosis. A comparison of the solutions has made it possible to indicate the parameters for which the solution for a multilayer solid can be replaced with sufficient accuracy by the solution for a single-layer cylinder. The obtained solutions can be used as a rough estimation when calculating the possible unknown parameters of the problem. Thus, the growth rate of an atherosclerotic plaque can be determined by using known stresses in the vessel wall, and vice versa, for a known rate of disease development, it is possible to determine the moment of occurrence of critical stresses in the vessel wall.

ACKNOWLEDGEMENTS

This work was supported by the Ministry of Science and Higher Education of the Russian Federation (state registration number AAAA-A20-120011690132-4) and RFBR projects (20-01-00666), and financial support of the SA (NRF) / RUSSIA (RFBR) joint science and technology research collaboration (project no. RUSA180527335500/19-51-60001).

CONFLICT OF INTEREST

The authors declare no potential conflict of interests.

ORCID

Evgenii V. Murashkin https://orcid.org/0000-0002-3267-4742
Evgeniy P. Dats https://orcid.org/0000-0003-1761-2911
Nikita E. Stadnik https://orcid.org/0000-0002-0187-8048

REFERENCES

1. Tennant M, McGeachie JK. Blood vessel structure and function: A brief update on recent advances. *ANZ J Surg*. 1990;60(10):747-753.
2. Folkman J. Angiogenesis. *Annu Rev Med*. 2006;57:1-18.
3. Logsdon EA, Finley SD, Popel AS, Gabhann FM. A systems biology view of blood vessel growth and remodelling. *J Cell Mol Med*. 2014;18(8):1491-1508. https://doi.org/10.1111/jcmm.12164
4. Goodger AM, Rogers PAW. Blood vessel growth in the endometrium. *Microcirc*. 1995;2(4):329-343. https://doi.org/10.3109/10739689509148277
5. Zahn A, Balzani D. A combined growth and remodeling framework for the approximation of residual stresses in arterial walls. *ZAMM*. 2018;98(12):2072-2100. https://doi.org/10.1002/zamm.201700273
6. Lee YT, Lin HY, Chan YWF, et al. Mouse models of atherosclerosis: A historical perspective and recent advances. *Lipids Health Dis*. 2017;16(1):12.
7. Mulvany MJ. Resistance vessel structure and the pathogenesis of hypertension. *J Hypertens Suppl: Off J Int Soc Hypertens*. 1993;11(5):S7-12.
8. Risau W. Mechanisms of angiogenesis. *Nature*. 1997;386(6626):671.
9. Zeev V, Edwards JE. Pathology of coronary atherosclerosis. *Prog Cardiovasc Dis*. 1971;14(3):256-274 english.
10. Furie B, Furie BC. Mechanisms of thrombus formation. *N Engl J Med*. 2008;359(9):938-949 english.
11. Bonadonna RC. The syndrome of insulin resistance and its links to atherosclerosis, International Textbook of Diabetes Mellitus. New York: John Willey & Sons; 2003. https://doi.org/10.1002/0470862092.d1009
12. Santoro L, Ferraro PM, Flex A, et al. New semiquantitative ultrasonographic score for peripheral arterial disease assessment and its association with cardiovascular risk factors. *Hypertens Research*. 2016;39(12):868.
13. Wu G, Yang J, Zhang T, et al. The diagnostic value of non-contrast enhanced quiescent interval single shot (QISS) magnetic resonance angiography at 3T for lower extremity peripheral arterial disease, in comparison to CT angiography. *J Cardiovasc Magn Reson*. 2017;18(1):71.
14. Kietselaer BLJH, Reutelingsperger CPM, Heidendal GAK, et al. Noninvasive detection of plaque instability with use of radiolabeled annexin A5 in patients with carotid-artery atherosclerosis. *N Engl J Med*. 2004;350(14):1472-1473.
15. Ihling C. Pathomorphology of coronary atherosclerosis. *Herz*. 1998;23(2):69-77 english.
16. Lim S, Park S. Role of vascular smooth muscle cell in the inflammation of atherosclerosis. *BMB Rep*. 2014;47(1):1.
17. Tabas I, García-Cardeña G, Owens GK. Recent insights into the cellular biology of atherosclerosis. *J Cell Biol*. 2015;209(1):13-22.
18. Ramsey SA, Gold ES, Aderem A. A systems biology approach to understanding atherosclerosis. *EMBO Mol Med*. 2010;2(3):79-89.
19. Wang D, Wang Z, Zhang L, Wang Y. Roles of cells from the arterial vessel wall in atherosclerosis. *Mediat Inflamm*. 2017;2017:8135934.
20. Taber LA. Biomechanics of growth, remodeling, and morphogenesis. *Appl Mech Rev*. 1995;48(8):487-545.
21. Humphrey JD. Continuum biomechanics of soft biological tissues. *Proc R Soc Lond Ser A: Math Phys Eng Sci*. 2003;459(2029):3-46.
22. Cowin SC. Tissue growth and remodeling. *Annu Rev Biomed Eng*. 2004;6:77-107.
23. Ogden RW, Holzapfel GA. *Mechanics of Biological Tissue*. Berlin Heidelberg: Springer-Verlag; 2006.
24. Cowin SC. The specific growth rates of tissues: a review and a re-evaluation. *J Biomech Eng*. 2011;133(4):041001.
25. Kuhl E. Growing matter: a review of growth in living systems. *J Mech Behav Biomed Mater*. 2014;29:529-543.
26. Epstein M. *The Elements of Continuum Biomechanics*. New York: John Wiley & Sons; 2012.
27. Goriely A. *The Mathematics and Mechanics of Biological Growth*, Vol. 45. New York, NY: Springer; 2017.
28. Southwell RV. *Introduction to the Theory of Elasticity for Engineers and Physicists*. Oxford: Oxford University Press; 1941.
29. Kovtanyuk LV, Murashkin EV. Onset of residual stress fields near solitary spherical inclusions in a perfectly elastoplastic medium. *Mech Solids*. 2009;44(1):79-87.
30. Burenin AA, Kovtanyuk LV, Murashkin EV. Strengthening of materials by intensive hydrostatic compression pretreatment. *Mech Solids*. 2012;47(6):665-670.
31. Murashkin EV, Dats EP. Thermoelastoplastic deformation of a multilayer ball. *Mech Solids*. 2017;52(5):495-500.
32. Murashkin EV, Dats EP. Coupled thermal stresses analysis in the composite elastic-plastic cylinder. *J Phys Conf Ser*. 2018;991:012060.
33. Hakobyan VN, Dats EP, Murashkin EV, Sahakyan AV. Contact stresses effects during plastic flow of thermoelastic-plastic multilayered spherical solids. In: IUTAM Symposium on Mechanical design and analysis for AM technologies. IPMech RAS; 2018; Moscow:12-16.
34. Hakobyan VN, Dats EP, Murashkin EV, Sahakyan AV. Residual stresses in assemblage of thermoplastic circular cylinders. In: IUTAM Symposium on Mechanical design and analysis for AM technologies. IPMech RAS; 2018b; Moscow:7-11.
35. Popov AL, Mironenko VN, Kozintsev VM, et al. Sample-free measurement of linear thermal expansion coefficient of aluminum-matrix composites using speckle-interferometry method. In: Proceedings of the World Congress on Engineering, Vol. 2. IAENG; 2018; London:767-772.
36. Rashba EI. Determination of stresses in the massive construction due to the action of its own weight taking into account the order of their erection. In: Sb. Tr. Inst. Stroit. Mekh. Ukr. Akad. Nauk, Vol. 18; 1953; Inst. Stroit. Mekh. Ukr. Akad. Nauk:23-27. (in Russian).
37. Kharlab VD. Linear theory of creep of a growing body. In: Mechanics of rod systems and continuous media: Tr. LISP, Vol. 49; 1966:93-119 (Russian). (in Russian).
38. Trincher VK. Formulation of the problem of determining the stress-strain state of a growing body. *Mech Solids*. 1984;19:119-124.
39. Bykovtsev GI, Lukanov AS. Some problems of the theory of solidifying and incrementing media. *Mech Solids*. 1985;20(5):112-115.
40. Arutyunyan NK, Naumov VE, Radaev YN. Dynamic build-up of the elastic layer. Part 1. Motion of a flow of deposited particles with a variable velocity. *Mech Solids*. 1992a;27(5):6-24.

41. Arutyunyan NK, Naumov VE, Radaev YN. Dynamic build-up of the elastic layer. Part 2. The case of the fall of the incrementing particles with a constant velocity. *Mech Solids*. 1992;27b(6):99-112.
42. Bykovtsev GI. Selected problems of mechanics of solids: Collected papers. Dal'nauka, (in Russian); 2002.
43. Kovalev VA, Radayev YN. On rationally complete algebraic systems of finite strain tensors of complex continua. *Izv Saratov Univ (NS), Ser Math Mech*. 2017;17:71-84 Russian. (in Russian).
44. Murashkin EV, Stadnik NE. Compatibility conditions in continua with microstrusture. *MATEC Web of Conf*. 2017;95:12001.
45. Manzhirov AV, Mikhin MN, Murashkin EV. Torsion of a growing shaft. *J Samara State Tech Univ, Ser Phys Math Sci*. 2017;221(4):684-698. (in Russian).
46. Stadnik NE, Dats EP. Continuum mathematical modelling of pathological growth of blood vessels. *J Phys Conf Ser*. 2018;991:012075.
47. Stadnik NE, Murashkin EV, Dats EP. Residual stresses in blood vessel wall during atherosclerosis. *AIP Conf Proc*. 2019;2116(1):380013.
48. Manzhirov AV, Murashkin EV, Parshin DA. Modeling of additive manufacturing and surface growth processes. *AIP Conf Proc*. 2019;2116(1):380011.
49. Murashkin EV, Radaev YN. On a differential constraint in asymmetric theories of the mechanics of growing solids. *Mech Solids*. 2019;54:1157-1164.
50. Murashkin EV, Radayev YN. On a differential constraint in the continuum theory of growing solids. *J Samara State Tech Univ, Ser Phys Math Sci*. 2019;23(4):1-11.
51. Zhilin PA, Altenbach H, Ivanova EA, Krivtsov A. *Material Strain Tensor*, Vol. 22. Berlin, Heidelberg: Springer; 2013.

How to cite this article: Murashkin EV, Dats EP, Stadnik NE. Application of surface growth model for a pathological process in a blood vessel's wall. *Math Meth Appl Sci*. 2020;1–16. https://doi.org/10.1002/mma.7056